International Journal of Technology 14(4) 833-842 (2023)
Received October 2022 / Revised December 2022 / Accepted April 2023

International Journal of Technology

http://ijtech.eng.ui.ac.id

Coating Material Development by Pulsed Laser Deposition for JIS SKD61 Steel Insert Pins Used in Aluminum Casting Industry

Rusman Kosasih[1*], Dedi Priadi[1], Maria Margaretha Suliyanti[2]

[1]*Material and Metallurgical Engineering Department, Faculty of Engineering, University of Indonesia, Depok, 16424, Indonesia*
[2]*Research Center for Photonics, National Research and Innovation Agency, South Tangerang, 15314, Indonesia*

Abstract. A Pulsed Laser Deposition (PLD) technique is a type of physical vapor deposition (PVD) technology. This research is one of a series of PVD studies aimed at determining the best PLD coating that can minimize the damage of steel pins made of SKD61 with a hardness of 48±1 HRc. The study began with the dummy blocks from SKD61 as research samples, followed by PVD-PLD with three coating materials as alternatives: Al/Cr (70:30), Al/Ti1 (50:50), and Al/Ti2 (63:37), all without active gases (N and C). The procedures used to test the research findings were FESEM, SEM, XRF, EDS, Vickers, and Rockwell Microhardness. The experiments were conducted at the BRIN Fotonic Research Center and the PT AHM Laboratory. The PLD process lasted for 10 minutes and employed an Nd: YAG laser with a wavelength of 1064 nm, a Q-switch with a time delay of 180 s, a pulse energy of 70 mJ, and a vacuum pressure of 1.161.35 Torr.Based on the results of the coating study, an AlTi1 coating was found to be the most effective material coating. The coating consisted of amorphous particles with a size range of 10 nm to 20 nm The coating had a thickness of 23 µm, and the surface hardness was measured to be 474-523 mHv for the single-layer coating and 477-501 mHv for the multilayer coating. The materials in both single-layer and multilayer coating samples have the same hardness in ascending order: AlCr, AlTi2, AlTi1, with a Ti concentration rise from 0.7% to 3.7%. The impact of the Ti element is also crucial in increasing hardness, wear resistance, and roughness.

Keywords: Coating material; Minimize damage; Pin SKD 61; PLD process

1. Introduction

Physical Vapour Deposition – Pulse Laser Deposition (PVD-PLD) is a coating process that has been widely used since 1987 to generate superconductive thin films with high-temperature resistance, which are employed in superconductors, medical applications, and electric, magnetic, and protective layers (Bruncko *et al.*, 2019; Duta and Popescu, 2019; Lorusso *et al.*, 2015; Krebs *et al.*, 2003). It is sensitive to the target condition, pulse energy, wavelength, vacuum process, target lens focus distance, and gas condition (Subramaniam, 2015). A typical PLD process experimental setup includes five key elements: target, substrate, laser, plasma plume, and vacuum condition (Masood, 2014). PLD has been developed in the last 10 years to manufacture crystalline layers for ceramic oxide, nitride films, and metallic multilayers, as well as to synthesize nanotubes, nanopowder, and quantum dots.

*Corresponding author's email: rusmankosasihsoehi@gmail.com, Tel.: +62-895-0745-3720
doi: 10.14716/ijtech.v14i4.6046

Pulse Laser Deposition – Neodymium-doped yttrium aluminum garnet (PLD-NdYAG) uses a laser beam to ionize the target material, which is then dispersed through a plasma arc generated during the laser irradiation process. The released ions are then deposited on a substrate as a thin layer made of 10-9 m nanosized particles, together with reactive gases (Katase *et al.*, 2012; Eason, 2007). Some physical and chemical material characteristics can change dramatically on the nanoscale from those of bulk-structured materials with the same composition. For example, the theoretical strength of nanomaterials can be achieved, or quantum effects can appear; nanosized crystals have a low melting point (up to a 1000°C difference with bulk structures) and reduced lattice constants because surface atoms or ions form a significant fraction of the total number of atoms or ions, and surface energy plays a significant role in thermal stability (Balaskas *et al.*, 2012; Katase *et al.*, 2012; Pokropivny *et al.*, 2007). Laser irradiance, Pulse Repetition Rate, and Liquid or Gas media also have important role for the deposition process (Khumaeni, Sutanto and Budi, 2019).

Scholars have been intrigued by current research and uses of superconductive materials, prompting them to investigate their potential usage for protective coatings (Yang *et al.*, 2018; Willmann *et al.*, 2008). Furthermore, the aluminum casting industry has seen an increase in the demand for protective layers to deal with die soldering. Die soldering occurs when aluminum welds to the dies or mold surface, leading to die damage and component defects and thereby halting production. Repairs are expensive and add more than an hour to production time. Die soldering is scientifically described as a chemical reaction that occurs during die casting between molten aluminum and the die surface. This reaction happens due to the washout or removal of a protective layer, such as a coating or lubricant, on the die. At sufficiently high temperatures and pressures, a protective layer is broken when liquid aluminum comes into contact with the die surface (Han, 2015). There are several alternatives method to minimize die soldering. Researchers have been studying to use of alloying material (Kohlhepp *et al.*, 2021), dies treatment method (Mochtar and Aldila, 2020), and coating method (Serekpayeva *et al.*, 2022; Kukuruzović *et al.*, 2021).

Han Qingyou and Viswanathan declare that coating the surface of the die is the most effective method to reduce soldering (Han and Viswanathan, 2003). The coatings must be resistant to molten aluminum corrosion (Saravanan *et al.*, 2018; Wang *et al.*, 2017; Dennis *et al.*, 2015; Presuel-Moreno *et al.*, 2008) and also oxidation (Pane *et al.*, 2023). The fluctuation of the solidus temperatures for an aluminum-iron-x system reveals that coatings comprising titanium (Ti), chromium (Cr), and manganese (Mn) are efficient for resisting molten aluminum because they tend to raise the critical temperature (TC) at which soldering occurs (Han and Viswanathan, 2003). Additionally, Studies suggest that TiN, CrN, and CrC coatings can create excellent physical barriers that prevent soldering in the aluminum casting industry. In addition, adding elements to the alloy that increase the thermal conductivity or decrease the liquid percentage can also reduce the occurrence of soldering. By performing thermodynamic analysis, other elements that increase thermal conductivity and serve as suitable coating materials can be identified.

Regarding the dimensional need of the automotive aluminum casting – machining component, which has a tolerance of +/- 50 μm, the PVD and CVD coating method became good alternatives because of their coating result, which max 20 μm thickness. PVD is chosen between these two methods because it has a lower working temperature, unnecessary to use toxic gases, has less process cost, and provides better coating properties (Oerlikon, 2012). PVD – PLD is being challenged to become a good alternative for a protective layer. This study attempts to determine which coating material has the highest performance for creating a protective layer on the surface of SKD 61 tool steel by using the PVD - PLD process.

2. Methods

2.1. Substrate

In the use of G4404-JIS hot work steel, steel plate samples (10 x 10 x 2 mm^2) manufactured of SKD61 (tool steels) were employed (Figure 1). The surface hardness acquired through heat treatment is in the 45-47 HRc range. This SKD61 tool steel is used for making several components of Dies such as cavity set, die/ mold base, slide core, ejector pin, ejector plate, and insert pin. These materials are supplied by PT Astra Honda Motor as the dies user. The samples were made by several steps. Milling using CNC Milling FANUC machine with rpm 2100, grinding using Surface grinding KURODA at rpm 2000, cutting using Cutting wheel METKON at rpm 1500, and polishing from # 600 until # 1000 using Polishing STRUERS machine with sandpaper.

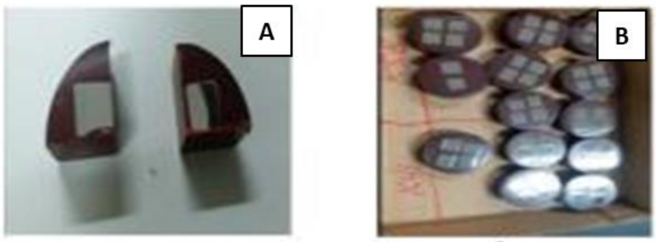

Figure 1 Steel plates SKD61 samples (a) single sample & (b) samples stock

2.2. Coating material variable

The steel plates were coated with three different materials supplied by PT Oerlikon Balzers Artoda Indonesia at different ratios: Al/Cr (70:30), Al/Ti (50:50), and Al/Ti (63:37) (Figure 2) utilizing two distinct coating processes, single-layer, and multilayer. Single-layer and Multilayer are referred to as the various products from PT Oerlikon. As the first step of coating continuous research, we will use all materials as is without any treatment for gas application. This is related to the vacuum chamber condition of PVD – PLD at the laboratory, which has no gas installation. For the next research, we will be going forward by using N_2 gas after the vacuum chamber modifying.

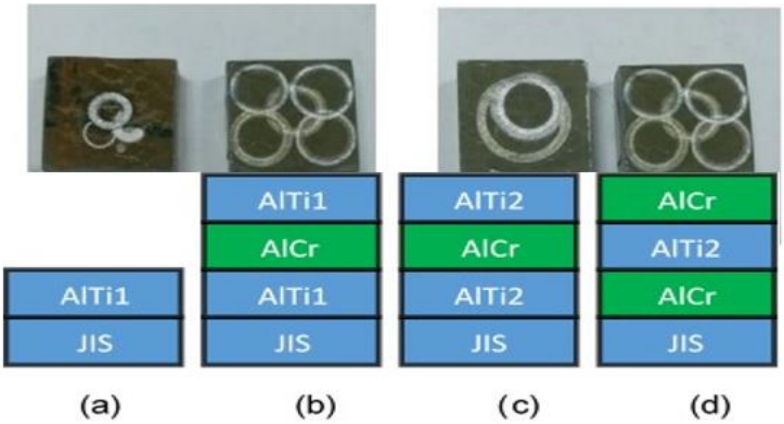

Figure 2 Samples of the two coating materials: AlCr and AlTi. a) single layer AlTi, b) multi-layer AlTi 50:50/ AlCr/ AlTi 50:50, c) multi-layer AlTi 63:37/ AlCr/ AlTi 63:37, (d) multi-layer AlCr/ AlTi 63:37/ AlCr

2.3. PLD Preparation

The PLD-NdYAG experiment was carried out at a wavelength of 1064 nm, with a pulse energy of 70 mJ, Q-switch after a time delay of 180 μs, a vacuum pressure of 1.16 ~ 1.35 Torr, and a lens focusing distance of 15 cm (Figure 3). These settings are determined through experiments to get the optimum setup outcomes as shown by plasma production in the target coating material. The good plasma is the one which has a 2- 3 mm flame dia, solid, and silent sound. To investigate the impacts, the materials were categorized such as A1 – A6 for single layer and A7 – A12 for multilayer. The experiments were conducted in a vacuum chamber with dimensions of 9 cm x 9 cm x 12 cm, using a 15 cm focus lens to enhance the strength of the laser strike. A rotary motor was used to maintain a target rotation speed of 3 rpm, while the target-substrate distance was set at approximately 1-1.5 cm.

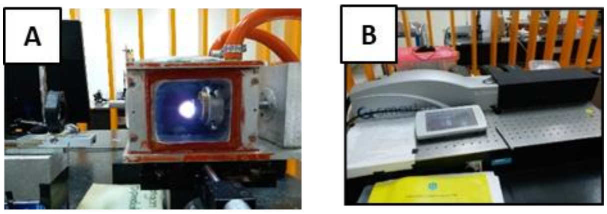

Figure 3 Laser plume: (a) 1064 nm wavelength, and (b) Laser Q smart 850

3. Results and Discussion

The samples were divided into groups to investigate the impacts of Al, Ti, and Cr and compare their alloy compositions with mechanical properties, i.e. the hardness of the coating layer (Figure 4). They were also divided into two groups based on coating processes (single-layer and multilayer) to see how the number of layers affected the same mechanical qualities. Table 1 shows the classification.

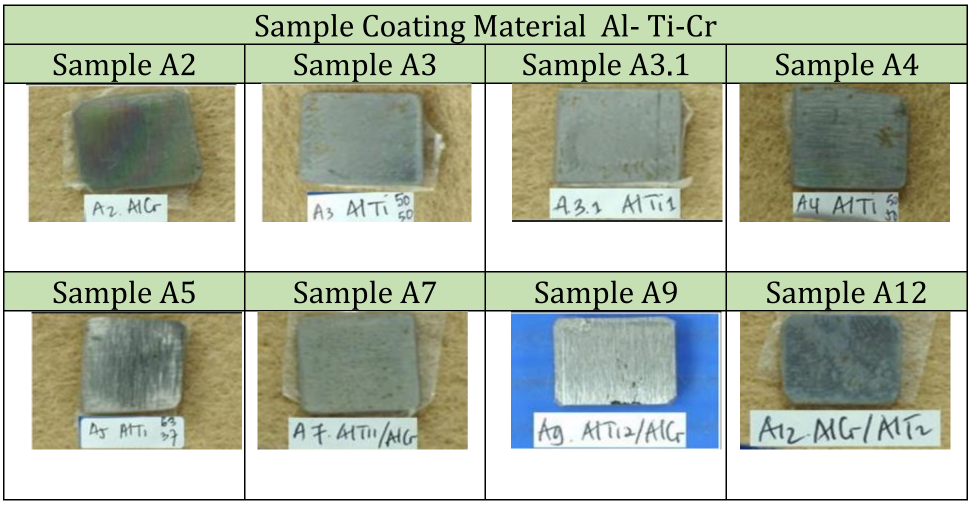

Figure 4 Visual examination of the SKD61 plates after PLD

Table 1 Sample grouping by coating materials and techniques

Coating Materials	Samples	Coating Techniques
Al/Cr (70:30)	A1, A2	Single-layer
Al/Ti1 (50:50)	A3, A4	Single-layer
Al/Ti2 (70:30)	A5, A6	Single-layer
Al/Ti1, Al/Cr, Al/Ti1	A7, A8	Multilayer
Al/Ti2, Al/Cr, Al/Ti2	A9, A10	Multilayer
Al/Cr, Al/Ti1, Al/Cr	A11, A12	Multilayer

3.1. FESEM test results

Field emission scanning electron microscopy (FESEM, FEI Helios Dual Beam) was used to study the microstructures of the PLD coatings at 10,000x, 20,000x, and 60,000x magnifications. FESEM images (Figure 5 and 6) reveal the presence of extremely tiny particles, 10–20 nm in size, with a thickness of 23 µm ~ 30 µm. This particle size is predicted to open up several opportunities to discover mechanical characteristics that differ from castings containing Al-Si particles with normal diameters of around 110 µm (Ishak *et al.*, 2017; Pokropivny *et al.*, 2007). In general, smaller sizes can have a bigger ratio of surface area vs volume than the normal size. In the end, it will bring more reaction at the surface of the nanoparticles (Ramahdita, 2011). Therefore, PLD may be used to create thin films, multilayers, nanotubes, nanofilaments, and nanosized particles (Christen and Eres, 2008). Furthermore, as shown in the cross-section of the coating, the coating film is 23 µm ~ 30 µm thick, defining it as a thin film.

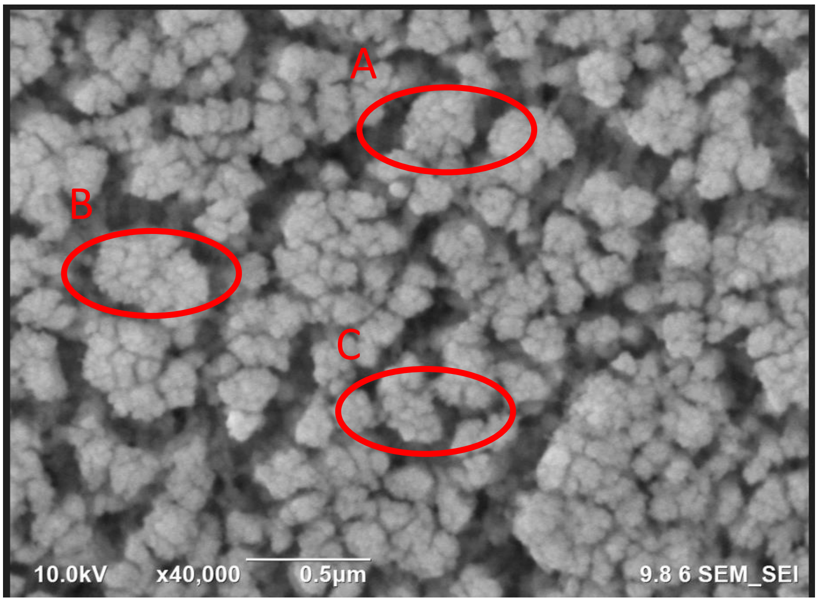

Figure 5 FESEM images of the PLD coatings (40,000x magnification): A = ±10 nm, B = ±20 nm, and C = ±20 nm

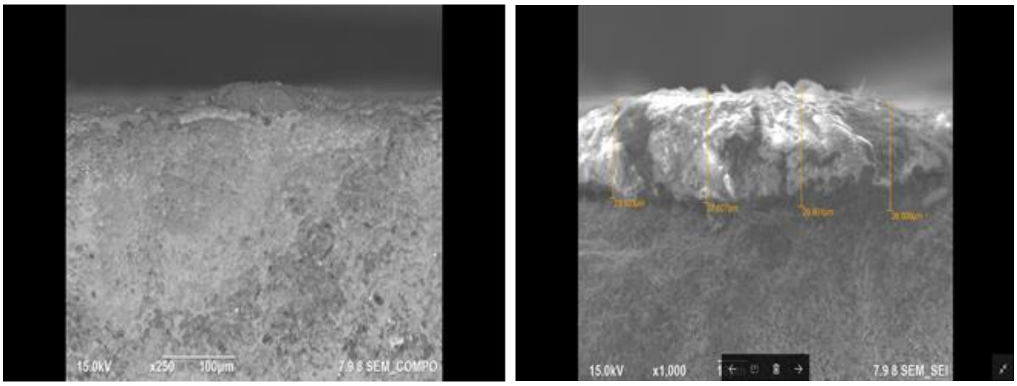

Figure 6 FESEM images showing the cross-section and thickness of the coating (250x and 1,000x magnifications)

3.2. XRF test results

The Oxford X-MET 3000TX was used for the X-ray fluorescence (XRF) test, and the findings were seen using the NIKON Epiphot 300 metallographic microscope. As shown in the Table 2. With an average weight of 91%, 10 Fe (basic metal) is discovered to be the main element. Similarly, Cr is the leading element in all of the investigated samples, although accounting for just 4.99% to 5% of the basic metal. Because of the lack of equipment capabilities and thickness of the coating film, Ti cannot be identified. Because the coating created is too thin, this composition is conceivable (Katase *et al.*, 2012); as a result, the detection process can penetrate the basic metal.

Table 2 Chemical compositions of the PLD coating samples, as identified in the XRF test

No	Sample	Composition (weight %)			
		Fe	Cr	Ti	Al
1	Sample A2	91.1	4.9	0	Not Defined
2	Sample A3	91.6	5.1	0	Not Defined
3	Sample A3.1	91	5	0	Not Defined
4	Sample A4	91.1	5.1	0.1	Not Defined
5	Sample A5	91	5	0.1	Not Defined
6	Sample A7	91.1	5	0.2	Not Defined
7	Sample A9	90.9	5.3	0	Not Defined
8	Sample A12	90.9	5	0.1	Not Defined

3.3. SEM-EDS test results

Analytical scanning electron microscope (SEM, JEOL JSM 6360 LA) observations reveal noticeable dark and bright lines on the coating. According to the EDAX Elect Plus energy dispersive spectroscopy (EDS) test, the bright lines (001) contain more Fe than their dark counterparts (002) (Figure 7). Both Cr and Ti content may be identified using the EDS and EDAX methods. Cr content is 0.9% and 5.4% by weight. While the Ti content is 0.7% and 3.7% by weight (Table 3).

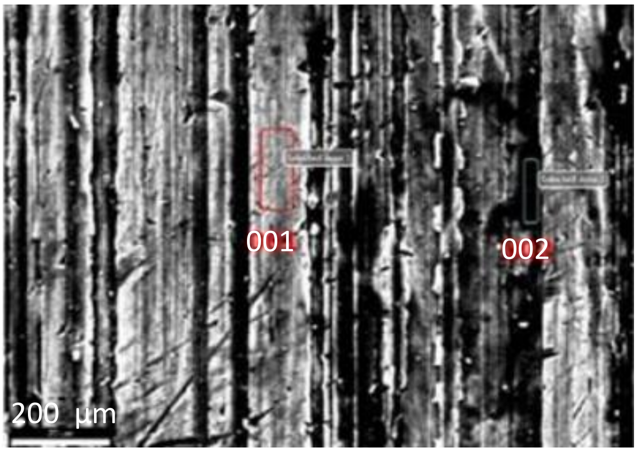

Figure 7 A noticeable dark and bright lines of the PLD coating samples, as identified in the SEM-EDS test

The titanium (Ti) content of the coated surface has a significant impact on its hardness, as shown in Figure 8 and Table 4. For the single layer type, the sample with the highest Ti concentration (1.65%, sample A3) exhibited a hardness value of 523 mHv, while the sample with the lowest Ti content (0.7%, sample A2) had a hardness of 474 mHv. In the case of the multi-layer type, the highest Ti concentration (2.6%, sample A7) resulted in a hardness value of 501 mHv, while the lowest Ti content (1.1%, sample A12) produced a hardness of 477 mHv. These results indicate that the greater the Ti percentage, the higher the hardness value of the coated layer (Çomaklı *et al.*, 2018). According to the hardness test findings, the ex-single-layer coating is harder than the ex-multilayer coating. In the meanwhile, another study revealed that multilayer coatings of varying thicknesses can increase performance (Vereschaka *et al.*, 2018).

Table 3 Chemical compositions of the PLD coating samples, as identified in the EDS test (EDAX Elect Plus)

No	Insert Pin		Chemical Composition By SEM-EDS (wt%)			
			Fe	Al	Ti	Cr
1	Sample A2	001	29.6	4.4	1.2	5.4
		002	3.1	10.9	0.7	3.2
2	Sample A3	001	39.6	2.2	1.1	4.7
		002	8.5	1.3	0.6	1.6
3	Sample A3.1	001	30.3	2.9	1.2	4
		002	3.2	5.5	3.7	1
4	Sample A4	001	32.3	3	1.5	4.7
		002	2.8	5.7	3.6	0.9
5	Sample A5	001	31.3	3.6	0.7	4
		002	16	2.4	0.9	2,3
6	Sample A7	001	39.3	4.5	2.2	4,2
		002	3.5	6.8	3	1.6
7	Sample A9	001	45.4	2.4	1.2	5
		002	2.4	5.6	1.3	1
8	Sample A12	001	14	4.6	1.1	3.1
		002	1.5	7.1	1.9	1.7

Table 4 Hardness, materials, and compositions of coating samples with different coating techniques

Samples	Ti (%)	mHv	Materials	Compositions
		Single-layer		
A3, A3.1, A4	1.65	523	Al/Ti1	50:50
A5	0.80	520	Al/Ti2	63:37
A2	0.70	474	Al/Cr	50:50
		Multilayer		
A7	2.60	501	Al/Ti1	Ti1/Cr/Ti1
A9	1.25	482	Al/Ti2	Ti2/Cr/Ti2
A12	1.10	477	Al/Cr	Cr/Ti/Cr

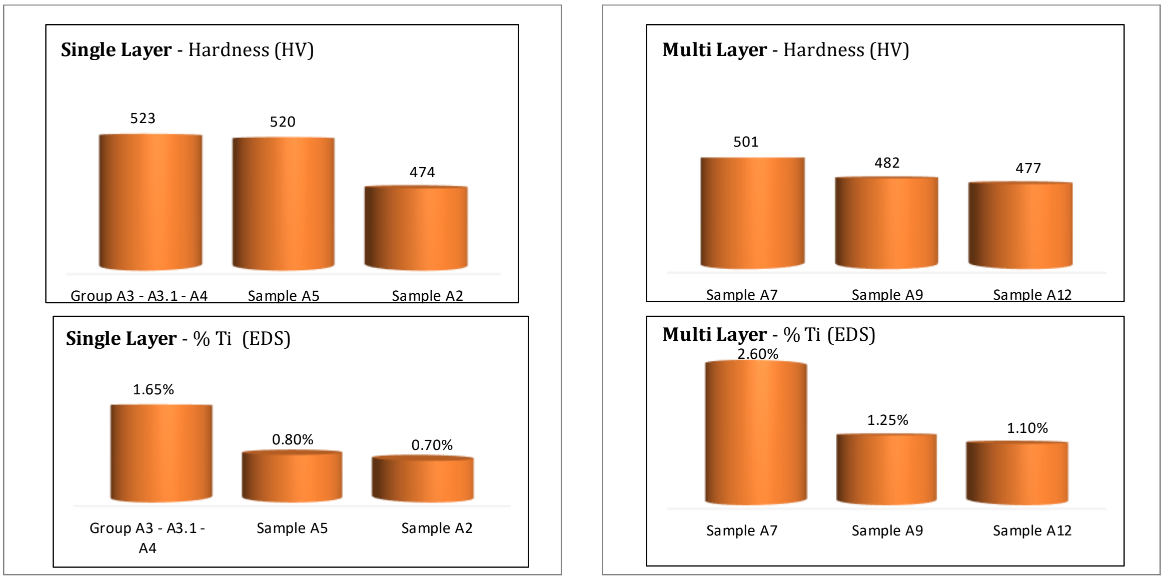

Figure 8 Vickers hardness test results of the single-layer and multilayer groups

3.4. VDI adhesion and roughness test results

The single-layer group's Rockwell hardness (FUTURE Tech FR-3EL) and SEM test results (Figure 9) revealed that Al/Ti1 (50:50) has higher adhesion performance and roughness than Al/Cr (70:30). Wear resistance shifts from HF1 (AlCr) to HF2 (AlTi), and roughness shifts from 0.051 m (AlCr) to 0.050 m. (AlTi). Adhesive level starts from good HF1 – HF4, up to bad HF5 - HF6. According to the findings of the adhesion and roughness tests, there is a close relationship between hardness, adhesiveness, and roughness, with Ti playing a substantial influence. Ti produces a tougher layer, which improves adhesive performance and roughness.

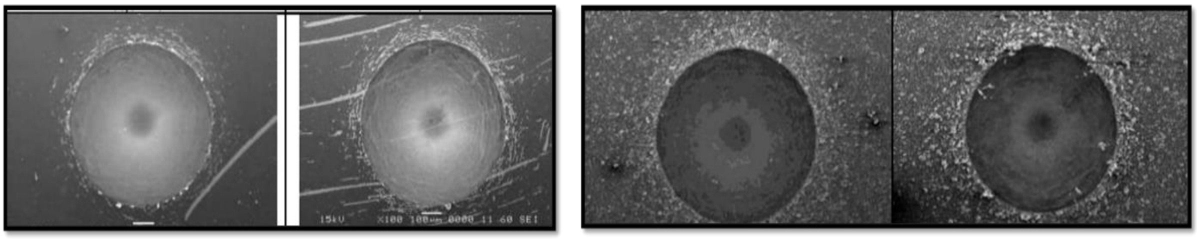

Figure 9 Adhesion performance and roughness of (a) AlCr 70/30 and (b) AlTi 50/50

Table 5 Adhesion Performance and roughness of AlCr 70/30 and AlTi 50/50

(a)

AlCr 70/30 : 180 mJ/20'		
Work	:	Roughness
Wavelenght	:	1064 nm
Date	:	04.Mar.20
Time	:	13:38:27
Adhesion	:	HF 1
Roughness	:	0.051 µm

(b)

AlTi 50/50 : 180 mJ/20'		
Work	:	Roughness
Wavelenght	:	1064 nm
Date	:	04.Mar.20
Time	:	13:44:18
Adhesion	:	HF 2
Roughness	:	0.05µm

4. Conclusions

With the parameter settings utilized in this work, the PLD-NdYAG method has been shown to be capable of creating a coating layer with nanosized particles, i.e. 10 - 20 nm. In this experiment, the former reached a maximum hardness of 523 mHv, while the latter had a maximum hardness of 501 mHv. Furthermore, the presence of Ti in the target material increases the hardness of the coating, in contrast to Cr. Ti has a hardness of up to 520 mHv in single-layer coating samples with a somewhat comparable composition, Al/X (65:35), whereas Cr has a hardness of 474 mHv. Material composition differences suggest that greater Ti concentrations in the coating are related to enhanced hardness. The coating materials in the single-layer samples are hardened in the following order: Al/Cr (70:30, 474 mHv), Al/Ti2 (63:37, 520 mHv), Al/Ti1 (50:50, 523 mHv). The metal surface adhesion and roughness test findings support the conclusion that Ti produces better-performing coatings than Cr. Al/Ti1 (50:50) has HF2 wear resistance and a Ra roughness of 0.050 m, whereas Al/Cr (70:30) has HF1 wear resistance and a Ra roughness of 0.051 m. As a result, further studies in the PVD research series are expected to meet the primary goal: the optimum coating to avoid die soldering of SKD61 insert pins.

Acknowledgments

The authors would like to express their appreciation to the University of Indonesia's Material and Metallurgical Engineering Department (postgraduate programme), the BRIN Fotonic Research Center, and PT AHM Laboratory for providing research opportunities and assistance during the experiment and characterization.

References

Balaskas, A.C., Kartsonakis, I.A., Tziveleka, L.-A. Kordas, G.C., 2012. Improvement of Anti-Corrosive Properties of Epoxy-Coated AA 2024-T3 with TiO_2 Nanocontainers Loaded With 8-Hydroxyquinoline. *Progress in Organic Coatings*, Volume 74(3), pp. 418–426

Bruncko, J., Šutta, P., Netrvalová, M., Michalka, M., Vincze, A., 2019. Pulsed Laser Deposition of Ga doped ZnO Films-Influence of Deposition Temperature and Laser Pulse Frequency on Structural, Optical and Electrical Properties. *Vacuum,* Volume 159, pp. 134–140

Christen, H.M., Eres, G., 2008. Recent Advances in Pulsed-Laser Deposition of Complex Oxides. *Journal of Physics: Condensed Matter,* Volume 20(26), p. 264005

Çomaklı, O., Yazıcı, M., Yetim, T., Yetim, A., Çelik, A., 2018. Effect of Ti Amount on Wear and Corrosion Properties of Ti-doped Al_2O_3 Nanocomposite Ceramic Coated CP Titanium Implant Material. *Ceramics International,* Volume 44(7), pp 7421–7428

Dennis, R.V., Patil, V., Andrews, J.L., Aldinger, J.P., Yadav, G.D., Banarjee, S., 2015. Hybrid Nanostructured Coatings for Corrosion Protection of Base Metals: A Sustainability Perspective, *Materials Research Express,* Volume 2(3), p. 032001

Duta, L., Popescu, A.C., 2019. Current Status on Pulsed Laser Deposition of Coatings from Animal-Origin Calcium Phosphate Sources, *Coatings,* Volume 9(5), p. 335

Eason, R., 2007. *Pulsed Laser Deposition of Thin Films: Applications-Led Growth of Functional Materials*. John Wiley & Sons

Han, Q., Viswanathan, S., 2003. Analysis of The Mechanism of Die Soldering in Aluminum Die Casting. *Metallurgical and Materials Transactions A,* Volume 34(1), pp 139–146

Han, Q.-Y., 2015. Mechanism of Die Soldering During Aluminum Die Casting. *China Foundry,* Volume 12(2), pp. 136–143

Ishak, N.N.M., Salleh, M.S., Yahaya, S.H., Mohamad, E., Sulaiman, M.A., 2017. The Effect of Equal Channel Angular Pressing (ECAP) on The Microstructure and Hardness of A356 Aluminium Alloy. *Journal of Advanced Manufacturing Technology,* Volume 11, pp 47–58

Katase, T., Hiramatsu, H., Kamiya, T., Hosono, H., 2012. Thin Film Growth by Pulsed Laser Deposition and Properties of 122-Type Iron-Based Superconductor AE (Fe1− xCox) 2As2 (AE= alkaline earth). *Superconductor Science and Technology,* Volume 25(8), p. 084015

Khumaeni, A., Sutanto, H., Budi, W.S., 2019. The Role of Laser Irradiance, Pulse Repetition Rate, and Liquid Media in the Synthesis of Gold Nanoparticles by the Laser Ablation Method using an Nd:YAG Laser 1064 nm at Low Energy. *International Journal of Technology*, Volume 10(5), pp. 961–969

Kohlhepp, M., Uggowitzer, P.J., Hummel, M., Hoppel, H.W., 2021 Formation of Die Soldering and the Influence of Alloying Elements on the Intermetallic Interface. *Materials*, Volume 14(7), p. 1580

Krebs, H.-U., Weisheit, M., Faupel, J., Süske, E., Scharf, T., Fuhse, C., Störmer, M., Sturm, K., Seibt, M., Kijewski, H., Nelke, D., Panchenko, E., Buback, M., 2003. Pulsed Laser Deposition (PLD)--a Versatile Thin Film Technique. In: *Advances in Solid State Physics.* Springer, pp 505–518

Kukuruzovic, D., Terek, P., Kovacevic, L, Škoric, B., Miletic, A., Panjan, P., Čekada, M., 2021. Investigation of CrAlN Coatings Soldering Resistance for High Pressure Die Casting Tools. *SVC Bulletin Fall/Winter 2021*, pp. 1–7

Lorusso, A., Gontad, F., Broitman, E., Chiadroni, E., Perrone, A., 2015. Characterisation of Pb thin Films Prepared by The Nanosecond Pulsed Laser Deposition Technique For Photocathode Application. *Thin Solid Films*, Volume 579, pp. 50–56

Masood, S.H., 2014. Advances in Fused Deposition Modeling. In: *Comprehensive Materials Processing*, pp. 69–91

Mochtar, M.A., Aldila, R., 2020. Die Soldering Behavior of H13 and Cr-Mo-V Tool Steel on die Casting Process on Nitriding-Shot Pinning Die Surface Treatment. *Materials Science Forum, 2020*, Volume 1000, pp 381–390

Oerlikon, P., 2012. *Technical Training Module*. Internal Company Course Training

Pane, J., Simbolon, D.H., Izzudin, H., Afandi, A., Hermanto, B., Sebayang, K., Humaidi, S., Situmorang, M., Sudiro, T., 2023. Cyclic Oxidation Resistance of MoSi2 Added FeCrAlTiY Coatings on ST41 Steel at 700°C Prepared by a Flame Spraying Technique. *International Journal of Technology,* Volume 14(1), pp. 15–25

Pokropivny, V., Lohmus, R., Hussainova, I., Pokropivny, A., Vlassov, S., 2007. *Introduction to Nanomaterials and Nanotechnology*. Ukraine: Tartu University Press

Presuel-Moreno, F., Jakab, M.A., Tailleart, N., Goldman, M., Scully, J.R., 2008. Corrosion-Resistant Metallic Coatings, *Materials Today,* Volume 11(10), pp. 14–23

Ramahdita, G., 2011. Karakterisasi Nanopartikel ZnO Hasil Sintesis Dengan Metode Presipitasi dan Perlakuan Pra-Hidrotermal (*Characterization of Synthesized ZnO Nanoparticles Using Precipitation Method and Pre-Hydrothermal Treatment*), Thesis, Graduate Program, Departement Teknik Metalurgi dan Material, Universitas Indonesia, Depok, p. 105

Saravanan, M., Devaraju, A., Venkateshwaran, N., Krishnakumari, A. Saarvesh, J., 2018. A Review on Recent Progress in Coatings on AISI Austenitic Stainless Steel. *Materials Today: Proceedings,* Volume 5(6), pp. 14392–14396

Serekpayeva, M., Niyazbekova, R., Al Azzam, K.M., Negim, E., Yeleussizova, A., Ibzhanova, A., 2022. Investigation of the Properties of Metallurgical Slags and Dust of Electro Filters to Obtain Protective Anticorrosive Coatings. *International Journal of Technology,* Volume 13(3), pp. 544–552

Subramaniam, T., 2015. 11 Pulsed Laser Deposition-DrVijayaRamnath-PDF Available online at: https://www.researchgate.net/publication/278672973_11_Pulsed_Laser_Depositi on-DrVijayaRamnath-PDF, Accessed on July 22, 2020

Vereschaka, A., Grigoriev, S., Sitnikov, N., Oganyan, G., Sotova, C., 2018. Influence of Thickness of Multilayer Composite Nano-Structured Coating Ti-TiN-(Ti, Al, Cr) N On Tool Life of Metal-Cutting Tool. *Procedia CIRP,* Volume 77, pp. 545–548

Wang, Z., Li, J., Wang, Y., Wang, Z., 2017 An EIS Analysis on Corrosion Resistance Of Anti-Abrasion Coating. *Surfaces and Interfaces*, Volume 6, pp 33–39

Willmann, H., Mayrhofer, P.H., Hultman, L., Mitterer, C., 2008. Hardness Evolution of Al–Cr–N Coatings Under Thermal Load. *Journal of Materials Research,* Volume 23(11), pp 2880–2885

Yang, T.S., Yao, S.H., Chang, Y.Y., Deng, J.H., 2018 Contact Behavior of Composite CrTiSiN Coated Dies in Compressing of Mg Alloy Sheets under High Pressure. *Materials,* Volume 11(1), p. 88